Fundamentals of graded ferroic materials and devices

Z.-G. Ban and S. P. Alpay
Department of Metallurgy and Materials Engineering and Institute of Materials Science, University of Connecticut, Storrs, Connecticut 06269

J. V. Mantese
Delphi Research Laboratories, Shelby Township, Michigan 48315

(Received 22 October 2002; revised manuscript received 21 January 2003; published 6 May 2003)

A generalized Landau-Ginzburg model is constructed and used to develop a methodology for analyzing graded ferroic materials. Material system inhomogeneities are assumed to arise from compositional, temperature, or stress gradients. These spatial nonuniformities are shown to give rise to local order parameters having corresponding spatial variation. Functionally graded ferroic systems are thus found to result in nonuniform free energies with attendant internal potentials, the latter of which are evidenced by displacements of the materials's stimulus-response hysteresis plots along the response axis (e.g., polarization, magnetization, or strain axis).

DOI: 10.1103/PhysRevB.67.184104 PACS number(s): 64.60.−i, 75.60.Ej, 77.80.−e

I. INTRODUCTION

Ferroics form an essential subgroup of functional (or smart) materials whose physical properties are sensitive to changes in external conditions such as temperature, pressure, electric, and magnetic fields. Ferroelectric, ferromagnetic, and ferroelastic materials are the best-known examples of ferroics that are principally distinguished by two main characteristics: First, their property-specific order parameters (e.g., polarization, magnetization, or self-strain, for ferroelectrics, ferromagnets, and ferroelastics, respectively) spontaneously assume nonzero values below a threshold temperature even in the absence of an applied stimulus. Thus these substances are usually high-energy–density materials that can be configured to store and release energy (electrical, magnetic, and mechanical) in well-regulated manners, making them highly useful as sensors and actuators. Second, ferroics (as a general class of materials) exhibit hysteresis in their stimulus-response behavior: e.g., polarization versus applied electric field, magnetization versus applied magnetic field, and strain versus applied stress.

While extensively studied both theoretically and experimentally, ferroic research has by and large been confined primarily to investigating the properties of homogeneous and layered materials. In recent years, however, an investigation of the properties of compositionally graded ferroelectric thin films has been undertaken.[1] Unlike homogeneous ferroelectrics, which are characterized by a symmetric hysteresis loop with respect to the polarization and applied field axes, graded ferroelectric devices display strikingly new behavior, the most notable being a translation of the hysteresis loop along the polarization axis with an attendant charge offset,[1–7] as shown in Fig. 1.

The ''up'' and ''down'' shifts observed in graded ferroelectric hysteresis have been shown to be dependant upon the degree of compositional gradient normal to the growth surface of the films. This behavior has been attributed to a ''built-in'' potential that finds its origin in the attendant polarization gradient that arises as the result of the compositional gradient. Such structures have given rise to a new class of transcapacitive ferroelectric devices (or ''transpacitors'') viewed to be the dielectric equivalent of semiconductor junction devices, having potential applications in infrared detection, actuation, and energy storage. Two types of graded ferroelectric device (GFD) structures have been demonstrated: ''up'' and ''down.''[2–5,8–10] This terminology arises from the fact that, unlike homogeneous ferroelectric materials, GFD yield ferroelectric charge-voltage hysteresis plots which are translated along the charge axis, up or down, when the GFD is placed in a modified Sawyer-Tower circuit and excited with a periodic alternating field.[2,5,9] Both types of devices have been formed from a wide variety of thin-film material systems,[2–5,8–11] though more recent research has shown that such translations are intrinsic in origin (having been replicated in bulk materials) and are not the result of extraneous artifacts.[7,12] However, while much is known experimentally concerning graded ferroelectric structures, theoretical descriptions and analysis of these or other transpacitive devices have been significantly lacking.

Considering the similarity of many ferroic systems, this report attempts to develop a common theoretical description for graded ferroic devices and structures. Starting from the generalized Landau-Ginzburg theory, we show that we can provide a quantitative theoretical analysis of the offset hysteresis behavior of polarization-graded ferroelectric materials. We also show that this approach is quite general and readily expandable to graded ferromagnets, ferroelastics, and other transponent and graded ferroic systems with proper modifications.

II. THEORY

Let us consider the expansion of the free energy of a ferroic phase transformation of a single-domain system with order parameters η_i such that it is a harmonic function of the order parameters (and thus does not contain odd powers):

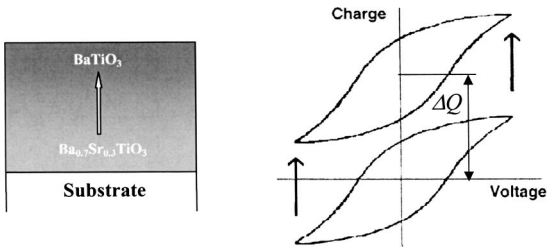

FIG. 1. Schematic of a compositionally graded barium strontium titanate film forming an ''up-'' graded ferroelectric stack and the corresponding asymmetric hysteresis loops with attendant charge offset ΔQ (see Refs. 1 and 2 for specific experimental details).

$$F(\eta_i)=\int_V\Big[\alpha_{ij}\eta_i\eta_j+\beta_{ijkl}\eta_i\eta_j\eta_k\eta_l+\cdots+A_{ijkl}(\nabla_i\eta_j\cdot\nabla_k\eta_l)+\delta_{ijk}x_{ij}\eta_k+\frac{1}{2}q_{ijkl}x_{ij}\eta_k\eta_l+\frac{1}{2}C_{ijkl}x_{ij}x_{kl}-\frac{1}{2}\Omega_i^D\eta_i-\Omega_i\eta_i\Big]dV, \tag{1}$$

where α_{ij}, β_{ijkl}, and A_{ijkl} are the free-energy expansion coefficients, δ_{ijk} and q_{ijkl} are the bilinear and linear-quadratic coupling coefficients between the order parameter and the strain x_{ij}, C_{ijkl} are the elastic coefficients, Ω_i is an externally applied electrical or magnetic field, and Ω_i^D is the internal depolarization or demagnetization field. Proper ferroelectric, ferromagnetic, and ferroelastic phase transformations can be described via the above relation with the polarization P_i, magnetization M_i, or the self-strain x_{ij}^0 as the order parameter, respectively. For a graded material with a systematic spatial variation in the order parameter, $\nabla_i\cdot\eta_j\neq 0$, resulting in a nonuniform (electric or magnetic) dipole moment density in ferroelectrics and ferromagnets and a nonuniform displacement in ferroelastic materials. It is this gradient which provides the basis for the offset of the hysteresis with respect to the applied electrical, magnetic, and stress fields.

To link with prior experimental results we confine our initial analysis to perovskite ferroelectric oxides such as $BaTiO_3$ which exhibit a cubic-tetragonal phase transformation. A systematic variation in the polarization can be achieved (and has been achieved experimentally) in a number of ways including a variation in the composition of the material,[2] impressing a temperature gradient across the structure,[12] or by imposing nonuniform external stress fields,[13] as illustrated in Fig. 2. For analysis, we consider a monodomain ferroelectric of thickness L sandwiched between two metallic electrodes with the easy axis of polarization along the z axis such that $P_1=P_2=0$, $P_3=P=f(z)$. The ferroelectric is assumed to be homogeneous along the x and y directions, reducing the problem to only one dimension. Accordingly, the general free energy expansion given in Eq. (1) reduces to the well-known Landau-Ginzburg-Devonshire (LGD) free energy per unit area:[14]

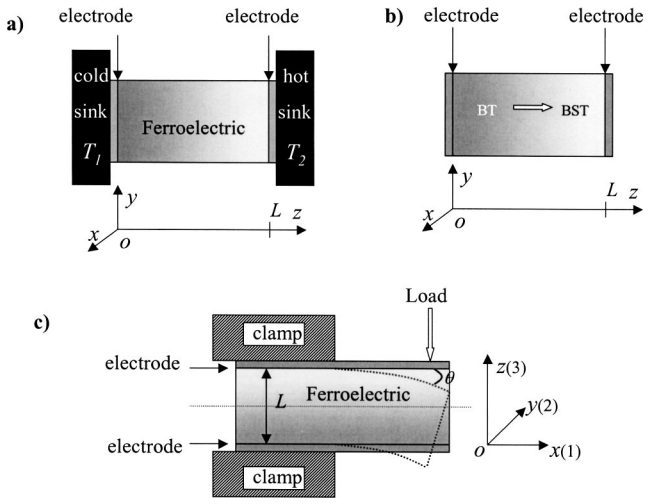

FIG. 2. Three methods of obtaining polarization graded ferroelectric materials: (a) temperature gradient, (b) compositional gradient (BT: $BaTiO_3$: BST: $Ba_xSr_{1-x}TiO_3$), and (c) strain gradient.

$$F=\int_0^L\Big[\frac{\alpha P^2}{2}+\frac{\beta P^4}{4}+\frac{\gamma P^6}{6}+\frac{A}{2}\Big(\frac{dP}{dz}\Big)^2-\frac{1}{2}E^DP-EP+F_{\rm el}^i\Big]dz. \tag{2}$$

where α, β, γ, and A are the free-energy expansion coefficients. The temperature dependence of the dielectric stiffness α is given by the Curie-Weiss law $\alpha=(T-T_0)/\varepsilon_0 C$, where T_0 and C are the Curie-Weiss temperature and constant, respectively, and ε_0 is the permittivity of free space. It is assumed that the coefficients β and γ do not depend on the temperature. The gradient term represents additional energy from the nonuniform distribution of the polarization and serves to damp out spatial variations in polarization.[14,15] The coefficient A can be approximated as $\delta^2|\alpha|$, where δ is the characteristic length along which the polarization varies. E is the external electric field along the z direction, and E^D is the depolarization field.[16] We assume that the contribution of the depolarization field is negligible due to the small but finite conductivity of the material as well as local compensation by defects such as oxygen vacancies in perovskite ferroelectrics. This term cannot be omitted in the analysis of ferromagnetic materials since there is no mechanism analogous to charge compensation in ferroelectrics.

The difference between the free-energy functional of Eq. (2) and the standard LGD free-energy expansion is the last term of Eq. (2): $F_{\rm el}^i$. It represents a contribution due to the internal stresses resulting from variation of the lattice parameter within the compositionally graded or temperature-graded unconstrained ferroelectric bar. The bar may be thought of being composed of ''layers'' with a uniform polarization along the z direction as shown in Fig. 3. There exists a biaxial stress state with equal orthogonal components in the xy plane of each layer, and the corresponding mechanical boundary conditions are given by $\sigma_1=\sigma_2$ and $\sigma_3=\sigma_4=\sigma_5=\sigma_6=0$, where σ_i are the components of the

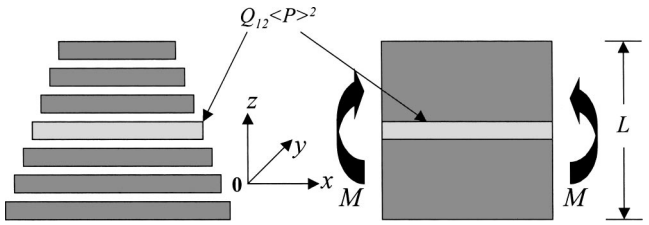

FIG. 3. Schematic diagrams showing the one-dimensional variation in the misfit between a particular ''layer'' and the layer with average self-strain given by $x^0(z)=Q_{12}[P^2(z)-\langle P\rangle^2]$. The self-strain results in a bending moment *M*.

internal stress tensor in the contracted notation. Thus the total internal elastic energy for each ''layer'' can then be expressed as

$$F_{\mathrm{el}}^i=\frac{1}{2}(\sigma_1 x_1+\sigma_2 x_2), \tag{3}$$

where $x_1=x_2$ and $\sigma_1=\sigma_2$ are the internal stresses and strains in the *xy* plane. The layer that has a polarization equivalent to the average polarization is distinguished by the light gray color in Fig. 3. The strain $x_1=x_2$ in each individual layer is given as[17]

$$x_1(z)=x_2(z)=x^0(z)+(z-L/2)\frac{\partial^2 w}{\partial x^2}=x^0(z)+(z-L/2)\kappa, \tag{4}$$

where *w* is the out-of-plane displacement. $x^0(z)$ represents the variation of the misfit in the *xy* plane between a particular layer and the average self-strain $Q_{12}\langle P\rangle^2$,

$$x^0(z)=Q_{12}[P^2(z)-\langle P\rangle^2], \tag{5}$$

where Q_{12} is the electrostrictive coefficient and $\langle P\rangle$ is the average polarization:

$$\langle P\rangle=\frac{1}{L}\int_0^L P(z)dz. \tag{6}$$

κ in Eq. (4) is the radius of curvature resulting from the bending moment given by[18]

$$\kappa=\frac{24}{L^3}\int_0^L (z-L/2)x^0(z)dz. \tag{7}$$

Combination of Eqs. (4)–(7) leads to

$$x(z)=x^0(z)+\frac{24(z-L/2)}{L^3}\int_0^L (z-L/2)x^0(z)dz, \tag{8}$$

and using the mechanical boundary conditions, the total internal elastic energy for each ''layer'' can then be expressed as

$$F_{\mathrm{el}}^i(z)=\frac{1}{2}(\sigma_1 x_1+\sigma_2 x_2)$$
$$=\overline{C}\{Q_{12}[P^2(z)-\langle P\rangle^2]+(z-L/2)\kappa\}^2, \tag{9}$$

where $\overline{C}$ is an effective elastic constant given by

$$\overline{C}=C_{11}+C_{12}-\frac{2C_{12}^2}{C_{11}}, \tag{10}$$

and C_{ij} are the elastic moduli at constant polarization.

The minimization of the free energy with respect to the polarization in the absence of an external electric field yields the Euler-Lagrange equation

$$A\frac{d^2P}{dz^2}=\overline{\alpha}P+\overline{\beta}P^3+\gamma P^5, \tag{11}$$

where the renormalized coefficients $\overline{\alpha}$ and $\overline{\beta}$ are given by

$$\overline{\alpha}=\alpha+4\overline{C}Q_{12}[(z-L/2)\kappa-Q_{12}\langle P\rangle^2], \tag{12}$$

$$\overline{\beta}=\beta+4\overline{C}Q_{12}^2. \tag{13}$$

The inhomogeneous nature of the three systems is reflected through the position-dependent expansion coefficients with respect to spatial temperature, composition, and strain variations. For compositionally graded ferroelectrics, $\overline{\alpha}$, $\overline{\beta}$, and *A* are a functions of the composition and therefore are location dependent [i.e., $\overline{\alpha}(z)$, $\overline{\beta}(z)$, and $A(z)$].

For temperature-graded ferroelectrics, *A* and $\overline{\alpha}$ depend on the temperature and thus are location dependent. Assuming that steady-state heat transfer is established [i.e., the temperature across the ferroelectric bar in Fig. 2(a) is a linear function of the position], the normalized coefficient $\overline{\alpha}(z)$ in Eq. (12) becomes

$$\overline{\alpha}(z)=\frac{L(T_1-T_0)+z(T_2-T_1)}{L\varepsilon_0 C}$$
$$+4\overline{C}Q_{12}[(z-L/2)\kappa-Q_{12}\langle P\rangle^2]. \tag{14}$$

The strain-graded ferroelectric is analyzed in terms of a simple cantilever beam setup [see Fig. 2(c)]. A bending force is applied along the *z* direction, resulting in a systematic variation along the *z* direction for the normal strain (compressive or tensile). The resulting stress conditions in the cantilever beam are $\sigma_1\neq 0$ and $\sigma_2=\sigma_3=0$. The coupling between the polarization and applied bending force modifies the Euler-Lagrange equation as follows:

$$A\frac{d^2P}{dz^2}=(\alpha-2Q_{12}C^*x_1)P+\beta P^3+\gamma P^5, \tag{15}$$

where

$$C^*=C_{11}-\frac{2C_{12}^2}{(C_{11}+C_{12})} \tag{16}$$

is the effective modulus in bending and $x_1(z)$ is the position-dependent normal strain due to the external bending force. The normal strain $x_1(z)$ is related to the bending angle θ and the length of the bended beam *S* through

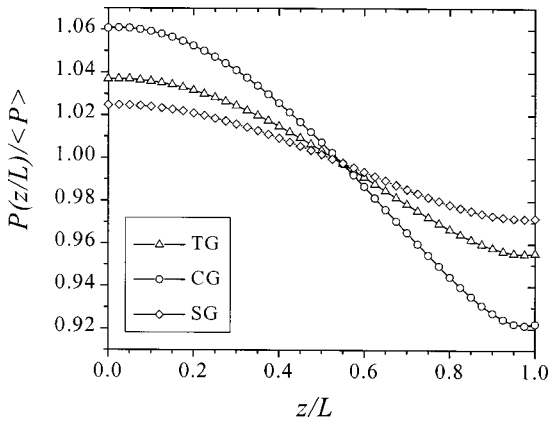

FIG. 4. Theoretical, normalized polarization profiles along the z direction for temperature- (TG), composition- (CG), and strain- (SG) graded systems.

$$x_1(z)=\left(z-\frac{L}{2}\right)\frac{\theta}{S}. \tag{17}$$

The polarization profile then can be used to calculate the charge offset per unit area ΔQ based on the one-dimensional Poisson's relation. Basic electrostatic theory shows that an inhomogeneous distribution of the polarization is associated with a bound charge:[19]

$$\rho_\nu=-\nabla_i\cdot P_j=-\frac{dP(z)}{dz}, \tag{18}$$

where ρ_ν is the volume density of the bound charge. According to Poisson's relation, this bound charge generates a built-in electrical field and the resulting built-in potential V_{int} is given by[3]

$$V_{\text{int}}=-\frac{1}{C_F L}\int_0^L z\rho_\nu(z)dz=\frac{1}{C_F L}\int_0^L z\left(\frac{dP(z)}{dz}\right)dz, \tag{19}$$

where C_F is the ferroelectric capacitance. Then, the charge offset due to this built-in potential is

$$\Delta Q=C_Q V_{\text{int}}=\frac{k}{L}\int_0^L z\left(\frac{dP(z)}{dz}\right)dz, \tag{20}$$

where k is the ratio of the capacitance of a load capacitor in Sawyer-Tower circuit C_Q to the capacitance of the graded ferroelectric C_F. It should be noted that in addition to the built-in electric field, there is built-in internal stress field due to the spatial variation of the polarization-induced self-strain.

III. RESULTS

Using the boundary conditions $dP/dz=0$ at $z=0$ and $z=L$ corresponding to complete charge compensation at the ferroelectric/electrode interfaces, we plot the polarization profile normalized with respected to the average polarization $\langle P\rangle$ for the three cases in Fig. 4. Here $P(z)$ is numerically obtained from Eqs. (11)–(17) using a finite-difference method having an accuracy of (successive iterations) approximately 10^{-7}. For the analysis we have chosen $BaTiO_3$ as the prototypical system for the temperature- and strain-graded ferroelectrics and $Ba_xSr_{1-x}TiO_3$ for the analysis of a compositionally graded ferroelectric system with $0<x<1$. The latter was selected primarily because there exists a great deal of information on the thermodynamic parameters and physical properties of $BaTiO_3$ and $SrTiO_3$. The coefficients α, β, and γ and the elastic constants C_{11} and C_{12} for $Ba_xSr_{1-x}TiO_3$ were obtained by averaging the corresponding parameters of $BaTiO_3$ and $SrTiO_3$ due to lack of thermodynamic data on single crystals of $Ba_xSr_{1-x}TiO_3$. For compositions close to $SrTiO_3$, it should be taken into account that upon cooling, bulk $SrTiO_3$ undergoes a cubic-to-tetragonal antiferrodistortive transition at $-168\,^\circ$C (105 K), well below the temperature range considered in this report. A ferroelectric transformation in stress-free $SrTiO_3$ crystals is not observed, but it is possible to induce ferroelectricity via external[20,21] and internal stresses.[22] The electrostrictive coefficients are assumed to be insensitive to variations in composition and temperature in the range of the analysis. Thermodynamic and physical properties of $BaTiO_3$ and $SrTiO_3$ used in the calculations are summarized in Table I.[22–26]

TABLE I. Thermodynamic and physical properties of $BaTiO_3$ and $SrTiO_3$ used in the calculations (compiled from Refs. 22–26, SI units, T in °C). Data for $Ba_xSr_{1-x}TiO_3$ are obtained by averaging the corresponding parameters of $BaTiO_3$ and $SrTiO_3$. The coefficient γ of $BaTiO_3$ is used for $Ba_xSr_{1-x}TiO_3$ as an approximation. The electrostrictive coefficient Q_{12} of $Ba_xSr_{1-x}TiO_3$ is assumed to have a typical value for perovskite oxides.

	$BaTiO_3$	$SrTiO_3$	$Ba_xSr_{1-x}TiO_3$
T_0	118	-253	$371x-253$
C	1.7×10^5	0.8×10^5	$(9x+8)\times10^4$
α	$6.65\times10^5(T-118)$	$1.41\times10^6(T+253)$	$1.12\times10^7(T-371x+253)/(9x+8)$
β	3.56×10^9	8.4×10^9	$(-11.96x+8.4)\times10^9$
γ	2.7×10^{11}		2.7×10^{11}
C_{11}	1.76×10^{11}	3.48×10^{11}	$(3.48-1.72x)\times10^{11}$
C_{12}	8.46×10^{10}	1.00×10^{11}	$(1-0.154x)\times10^{11}$
Q_{12}	-0.043		-0.034

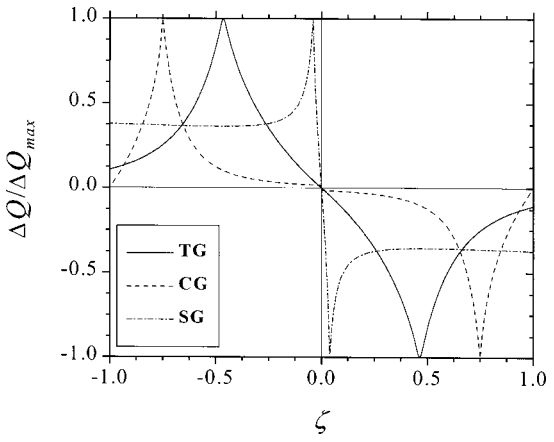

FIG. 5. Normalized charge offset as a function of the parameter ζ for temperature-graded BT, $\zeta=\Delta T/|\Delta T|_{\max}$ (TG); compositional-graded BST, $\zeta=C_{\mathrm{Ba}}$ (CG); and strain-graded BT, $\zeta=\theta/|\theta|_{\max}$ (SG).

As can be seen from Fig. 4, the normalized polarization decreases monotonically across the structure with a variation of the polarization along the z direction predicted in all three graded systems. The polarization gradient diminishes close to the surfaces because of the boundary conditions. For the temperature-graded $BaTiO_3$ system, the hot end and cold end are chosen to be at T_0 (Curie-Weiss temperature) and room temperature (RT$=25\,^{\circ}$C), respectively. If the hot-end temperature is higher than T_0, a paraelectric region with no spontaneous polarization will form at this end, a feature important for analyzing the charge offset behavior with respect to the temperature as well. Within the ferroelectric region, the polarization profile exhibits similar behavior as the one shown in Fig. 4. The end-point compositions for compositionally graded systems are $BaTiO_3$ (at $z=0$) and $Ba_{0.75}Sr_{0.25}TiO_3$ (at $z=L$), respectively, and a linear relationship between the composition and position is assumed. It is worth mentioning that the magnitude and direction of the polarization gradient depend upon the temperature, composition, and strain gradient. For example, the direction of the polarization gradients will be reversed if the positions of the hot- and cold-heat sinks in Fig. 2(a) are exchanged. In the strain-graded $BaTiO_3$ system, the deflection angle θ of the level arm is taken as 1.5°. A more abrupt polarization gradient should be expected with increasing θ.

In Fig. 5 we plot the charge offset $\Delta Q/\Delta Q_{\max}$ as a function of the normalized parameter ζ for three cases. For temperature-graded $BaTiO_3$, ζ is defined as $\zeta=\Delta T/|\Delta T|_{\max}$, where $\Delta T=T_2-T_1$ ($T_1=$RT and T_2 is a variable for positive ζ, vice versa for negative ζ). It can be seen from Fig. 5 that the charge offset first increases in a continuous fashion with increasing ζ, reaching a maximum corresponding to $T_2=T_0$, and then decreases. Further increase in the temperature leads to the formation of a paraelectric region within the ferroelectric bar with no spontaneous polarization. This region expands with increasing T_2, reducing the charge offset. This very same trend has been observed experimentally in temperature-graded $Ba_{0.7}Sr_{0.3}TiO_3$.[12]

A similar behavior is predicted for compositionally graded $Ba_xSr_{1-x}TiO_3$ and strain-graded $BaTiO_3$. For compositionally graded $Ba_xSr_{1-x}TiO_3$, ζ is defined as the Ba concentration on one end of the ferroelectric (i.e., this end has the composition of pure $BaTiO_3$ when $\zeta=1$ and has the composition of pure $SrTiO_3$ when $\zeta=0$), and the other end has a fixed concentration corresponding to pure $BaTiO_3$. $\zeta<0$ corresponds to reversed grading. For strain-graded $BaTiO_3$, ζ is the normalized bending angle $\theta/|\theta|_{\max}$, where $|\theta|_{\max}$ is the maximum bending angle. For compositionally homogeneous ($\zeta=1$) or unbent ferroelectric bars ($\zeta=0$), there is no charge offset. A maximum charge offset is predicted at a critical ζ in both cases, corresponding to the emergence of a paraelectric region. However, a steady increase of the charge offset is theoretically expected for relatively larger bending angles in strain-graded $BaTiO_3$ due to the saturation of the expansion of the paraelectric region in tensile strain regime and a continuously increasing polarization gradient in the compressive strain regime. An important feature predicted by the model is that the sign of the charge offset is reversed if that of the temperature, composition, or strain grading is reversed, as shown in the negative-ζ regions in Fig. 5 justifiable with the same kind of reasoning as discussed for positive ζ.

IV. DISCUSSION AND CONCLUSIONS

Although hysteresis offsets have been observed from temperature- or strain-graded ferroelectric systems, the majority of the research on graded ferroelectrics has concentrated on compositionally graded ferroelectrics. The theoretical modeling for many compositionally graded systems depends on the availability of thermodynamic data and physical properties of single crystals of not just the end components, but in between solid solutions as well. Furthermore, there are additional factors that have to be taken into account when polycrystalline materials, polycrystalline thin films, and epitaxial thin films are considered. For thin films (whether they are polycrystalline, textured, or epitaxial) the clamping effect of the substrate, which is usually much thicker than the film, has to be considered.[23,27] In addition, the coupling of the internal stresses with the self-strain of the phase transformation and thus with the polarization through the electrostrictive effect should also be taken into account.[23,27] There are several sources of internal stresses in thin films: the structural phase transformation at the Curie temperature, the difference in the thermal expansion coefficients of the film and the substrate, and lattice mismatch between the layers in the case of epitaxial films. It is expected that the combination of the nonuniform internal stresses in graded thin films with F^i_{el} should complicate the analysis in computing the magnitude of the hysteresis offset.[8,13]

While the analysis presented in this report explored the properties of graded ferroelectrics, the findings are quite general and apply equally well to other ferroic material systems such as ferromagnets and ferroelastics with proper modifications of the free-energy function. Indeed, substitution of any other equally acceptable order parameter into Eq. (1) will yield a spatially dependent free energy and attendant internal

potential. For example, the ferromagnetic state can be described via the Landau potential, taking into account the exchange energy, magnetic anisotropy, magnetostriction, demagnetization energy, and magnetostatic energy. Either the magnetization or self-strain of the transformation can be chosen as the order parameter. For pure ferroelastic transformations, the potential is seemingly simpler due to the absence of the coupling of the polarization or magnetization with the self-strain, which is the order parameter. However, the direct effect of internal strains as described via Eq. (8) in compositionally graded and temperature-graded systems as well as the strains resulting from the bending in strain-graded systems on the self-strain has to be taken into account. A systematic variation in the magnetization or the self-strain as predicted in our model should result in a nonuniform magnetic dipole moment density or a nonuniform displacement (resulting in, for example, external bending[18]) in ferroelastic materials constituting the basis of the offset of the hysteresis with respect to the stimulus. Unlike passive and homogeneous ferroics, transpacitors, transductors, translastics, and other transponent devices (formed from nonhomogeneous ferroics) are active devices with potential applications in a multitude of high-sensitivity, high-energy-applications: sensors, actuators, and other energy storage and metering devices. Until this present work, there has not been any attempt to undertake a general analysis of nonhomogeneous ferroics. This work provides the basic fundamentals related to these active structures, thereby enabling predictive capabilities for new transponent configurations.

ACKNOWLEDGMENTS

We gratefully acknowledge helpful conversations with N. W. Schubring and A. L. Micheli of Delphi Research Laboratories and A. L. Roytburd of the University of Maryland. Z.-G.B. and S.P.A. also wish to acknowledge support from the National Science Foundation (NSF) under Grant No. DMR-0132918 and the University of Connecticut Research Foundation.

[1] N. W. Schubring, J. V. Mantese, A. L. Micheli, A. B. Catalan, and R. J. Lopez, Phys. Rev. Lett. **68**, 1778 (1992); J. V. Mantese and N. W. Schubring, Integr. Ferroelectr. **37**, 245 (2001).
[2] J. V. Mantese, N. W. Schubring, A. L. Micheli, M. S. Mohammed, R. Naik, and G. W. Auner, Appl. Phys. Lett. **71**, 2047 (1997).
[3] Z. Chen, K. Arita, M. Lim, and C. A. P. Araujo, Integr. Ferroelectr. **24**, 181 (1999).
[4] M. Brazier, M. McElfresh, and S. Mansour, Appl. Phys. Lett. **72**, 1121 (1998).
[5] D. Bao, X. Yao, and L. Zhang, Appl. Phys. Lett. **76**, 2779 (2000).
[6] D. Bao, N. Mizutani, X. Yao, and L. Zhang, Appl. Phys. Lett. **77**, 1203 (2000).
[7] D. Bao, N. Wakiya, K. Shinozaki, N. Mizutani, and X. Yao, J. Appl. Phys. **90**, 506 (2001).
[8] T. Tsurumi, T. Miyasou, Y. Ishibashi, and N. Ohashi, Jpn. J. Appl. Phys., Part 1 **37**, 5104 (1998).
[9] D. Bao, N. Mizutani, X. Yao, and L. Zhang, Appl. Phys. Lett. **77**, 1041 (2000).
[10] I. Boerasu, L. Pintilie, and M. Kosec, Appl. Phys. Lett. **77**, 2231 (2000).
[11] J. V. Mantese, N. W. Schubring, A. L. Micheli, and A. B. Catalan, Appl. Phys. Lett. **67**, 721 (1995).
[12] W. Fellberg, J. V. Mantese, N. W. Schubring, and A. L. Micheli, Appl. Phys. Lett. **78**, 524 (2001).
[13] J. V. Mantese, N. W. Schubring, A. L. Micheli, M. P. Thompson, R. Naik, G. W. Auner, I. B. Misirlioglu, and S. P. Alpay, Appl. Phys. Lett. **81**, 1068 (2002).
[14] L. D. Landau and E. M. Lifshitz, *Statistical Physics* (Pergamon, Oxford, 1980).
[15] L. P. Kadanoff, W. Gotze, D. Hamblen, R. Hecht, E. A. S. Lewis, V. V. Paiciauskas, M. Rayl, J. Swift, D. Aspnes, and J. Kane, Rev. Mod. Phys. **39**, 395 (1967).
[16] R. Kretschmer and K. Binder, Phys. Rev. B **20**, 1065 (1979).
[17] M. Finot and S. Suresh, J. Mech. Phys. Solids **44**, 683 (1996).
[18] See the Appendix in A. L. Roytburd and J. Slutsker, Acta Mater. **50**, 1809 (2002).
[19] B. A. Strukov and A. P. Levanyuk, *Ferroelectric Phenomena in Crystals* (Springer-Verlag, Berlin, 1998).
[20] J. C. Slonczewski and H. Thomas, Phys. Rev. B **1**, 3599 (1970).
[21] H. Uwe and T. Sakudo, Phys. Rev. B **13**, 271 (1976).
[22] N. A. Pertsev, A. K. Tagantsev, and N. Setter, Phys. Rev. B **61**, R825 (2000).
[23] N. A. Pertsev, A. G. Zembilgotov, and A. K. Tagantsev, Phys. Rev. Lett. **80**, 1988 (1998).
[24] B. D. Qu, W. L. Zhong, and R. H. Prince, Phys. Rev. B **55**, 11 218 (1997).
[25] K. A. Muller and H. Burkhard, Phys. Rev. B **19**, 3593 (1979).
[26] T. Yamada, J. Appl. Phys. **43**, 328 (1972).
[27] A. L. Roytburd, S. P. Alpay, V. Nagarajan, C. S. Ganpule, S. Aggarwal, E. D. Williams, and R. Ramesh, Phys. Rev. Lett. **85**, 190 (2000).